

# PERFORMANCES OF SPIRAL2 LOW AND HIGH BETA CRYOMODULES

C. Marchand\*, P. Bosland, G. Devanz, O. Piquet, CEA, Saclay, France  
 D. Longuevergne, G. Olry, IPN, Orsay, France  
 Y. Gómez Martínez, LPSC, Grenoble, France  
 P.-E. Bernaudin, R. Ferdinand, GANIL, Caen, France

## Abstract

All SPIRAL2 cryomodules (twelve with one quarter wave resonator (QWR) at  $\beta=0.07$  and seven with two QWRs at  $\beta=0.12$ ) have been produced and qualified, and are now in installation phase on the LINAC at GANIL. After a general introduction on the LINAC, we will first remember and compare the different design choices taken for the two families of cryomodules. We will then present a summary of the techniques used for the preparation and integration of the cavities in the cryomodules, and compare the achieved performances with design parameters. At last, we describe the status of the LINAC installation as of end of August 2015.

## INTRODUCTION

The GANIL's SPIRAL 2 Project [1] aims at delivering high intensities of rare isotope beams by adopting the best production method for each respective radioactive beam. The unstable beams will be produced by the ISOL “Isotope Separation On-Line” method via a converter, or by direct irradiation of fissile material.

The driver will accelerate protons (0.15 to 5 mA –33 MeV), deuterons (0.15 to 5 mA – 40 MeV) and heavy ions (up to 1 mA,  $Q/A=1/3$  14.5 MeV/u to  $1/6$  8.5 MeV/A). It consists of high performance ECR sources, a RFQ, and the superconducting light/heavy ion LINAC. The driver is also asked to provide all the energies from 2 MeV/u to the maximum designed value (see Table 1).



Figure 1: SPIRAL2 LINAC – 2 QWR families.

The SPIRAL2 [1] LINAC is based on superconducting (SC), independently phased resonators (Fig. 1). In order to allow the broad required ranges of particles, intensities and energies, it is composed of two families of short cryomodules developed by CEA/Irfu and IN2P3/IPN-O teams. The first family (CMA) is composed of 12 quarter-wave resonators (QWR) with  $\beta_0=0.07$  (one cavity/cryomodule), and the second family (CMB) of 14 QWR at  $\beta_0=0.12$  (two cavities/cryomodule) (see Fig. 4). Resonance frequency is 88.0525 MHz and maximum gradient in operation of the QWRs is  $E_{acc} = V_{acc}/\beta\lambda = 6.5$  MV/m. The exact values of accelerating field used in each cavity for different ion species is illustrated on Fig. 2, which is the result of beam dynamics studies to optimize longitudinal focalization and acceptance of the ion beam [2].

SRF Technology - Cavity

E07-Non-Elliptical performance

Developed by IN2P3/LPSC (Grenoble), the RF power couplers shall provide up to 12 kW CW beam loading power to each cavity [3]. The transverse focusing is ensured by means of warm quadrupole doublets located between each cryomodule, in so-called “warm sections” also equipped with beam diagnostic and vacuum equipments (see Fig. 3).

Table 1: Beam Specifications

Particles	H <sup>+</sup>	<sup>3</sup> He <sup>2+</sup>	D <sup>+</sup>	ions	ions
Q/A	1	3/2	1/2	1/3	1/6
Max. I (mA)	5	5	5	1	1
Min. energy (MeV/A)	0.75	0.75	0.75	0.75	0.75
Max energy (MeV/A)	33	24	20	15	9
Max. beam power (kW)	165	180	200	45	54

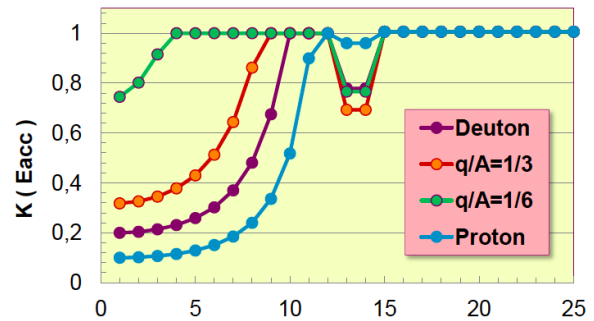


Figure 2: Ratio  $K =$  cavity accelerating field/max accelerating field for different beam types in the LINAC.

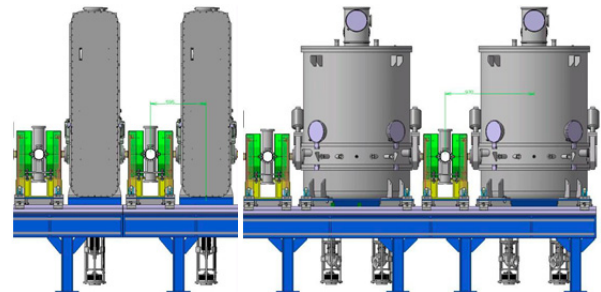


Figure 3: The warm quadrupoles (in green) installed between the cryomodules (left: CMA; right: CMB).

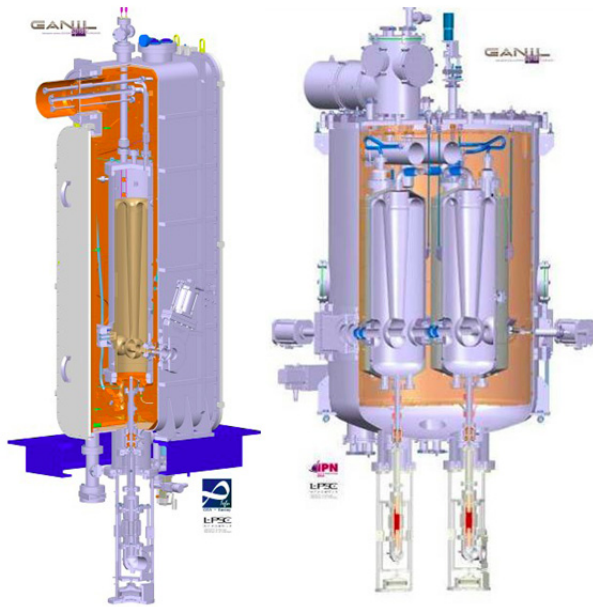


Figure 4: The SPIRAL2 cryomodules (left: CMA  $\beta_0=0.07$ ; right: CMB  $\beta_0=0.12$ )

## CAVITIES AND CRYOMODULES DESIGN

SPIRAL2 cryomodules design has been described in detail in previous papers [4][5][6], and the full history of changes between prototypes and series in [7].

They are both short cryomodules (one or two cavities per cryomodule, see Fig. 4) with no solenoid inside. Cavities are bulk niobium, quarter-wave resonators (see Fig. 5 and Table 2).

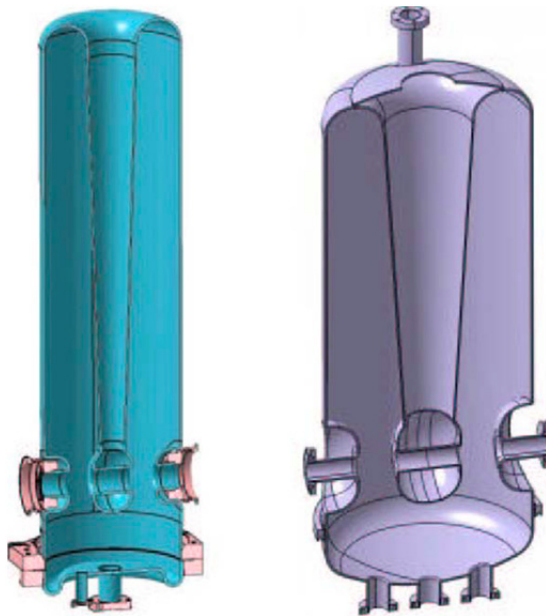


Figure 5:  $\beta_0=0.07$  (left) and  $\beta_0=0.12$  (right) QWRs.

Table 2: Characteristics of  $\lambda/4$  Cavities

Frequency (MHz)	88.05	88.05
$\beta_0$	0.07	0.12
$E_{pk}/E_{acc}$	5.0	5.6
$B_{pk}/E_{acc}$ (mT/MV/m)	8.9	10.2
$r/Q$ ( $\Omega$ )	631	518
$V_{acc}$ at 6.5 MV/m (MV)	1.54	2.65
$G$ ( $\Omega$ )	22.4	38
Beam tube $\phi$ (mm)	30	36
Cavity ext. $\phi$ (mm)	230	380
$Q_{ext}$	$6.6 \times 10^5$	$1.1 \times 10^6$

Cavities are cylindrical in shape and the inner stem is conical, with toric stem-to-body top. The helium jacket doesn't cover the bottom part of the cavities. Insulation vacuum and beam vacuum are separated. Cavities are operated at 4 K, and the copper thermal screen is cooled at 60 K using 15 bar He gas.

Power coupler is of the fixed type, located on the bottom plate of cavities. Couplers are similar for both types of cavities. Coupling factor is optimized for each family of cryomodules ( $5.5 \cdot 10^5$  for low beta cavities and  $1.1 \cdot 10^6$  for high beta cavities), considering the peak intensities of the various particles to be accelerated by the LINAC.

Detailed design of both cryomodules and cavities families has been performed independently in two different laboratories, with only minimal standardization (power couplers being one of the few common components). We will now describe some specific design choices that are somewhat different for both cavities and cryomodules type, and explain the rationale behind the choices.

### Low-beta Cryomodules Specificities

Low beta cavities are closed by a removable bottom plate made of OFHC copper, intended to ease HPR cleaning of these small cavities.

Tuning system is mechanical. Deformation of the cavities by squeezing its outer body perpendicularly to the beam axis provides a 13 kHz tuning range.

Magnetic shielding is made of room temperature, MuMetal plates located against the outer vessel.

Cavity position is adjusted and aligned while the cryomodule is open, and fiducial marks reported on the outside of the cryomodule allow to keep this alignment on the LINAC.

### High-beta Cryomodules Specificities

High beta cavities have no removable bottom, all niobium parts of the cavity are electron welded. HPR is possible through two entry feeds located on top of the cavities.

Tuning is performed by a niobium plunger, moving up and down inside the cavity. This system, located on top of the cavity in the maximum magnetic field area, provides a tuning range of slightly more than 10 kHz.

Magnetic shielding is located against the cavities and made of Cryophy material. It is cooled by the same circuit as the cavity, to ensure that the permeability of the material is as high as possible when niobium transits to the SC state.

Windows, sights and rods allow checking and adjusting the cavity alignment both at room and at cold temperature, the specifications being that when cooled down, the cavities are aligned on the beam axis within 1 mm.

### CAVITIES AND CRYOMODULES PREPARATION AND ASSEMBLY

Both families of cavities are prepared using standard BCP chemical treatments, followed by 18MΩ water high pressure rinsing (HPR) in clean room. None have been heat cured against 100 K effect. High beta cavities are baked while under vacuum in clean room (120°C for 48h). This baking proved to enhance  $Q_0$  by 50% (mean value) [8]. This effect was not observed on low beta cavities, as a large part of the RF surface resistance  $R_s$  of the cavity is dominated by the copper bottom plate, which does not benefit from the baking.

The quality factor  $Q_0$  of the pre-series low beta cavities was one order of magnitude below specifications. Extensive analysis and testing helped solving the problem, related to the bottom plate and flange [8]. The indium seal retained at the end not being easy to remove, it was decided not to HPR rinse the cavities between the vertical cryostat (VC) test and assembling inside the cryomodule. This is the standard procedure finally used on the series cavities, which proved completely satisfactory [9].

In the series assembling of the first three high beta cryomodules, none of them achieved the nominal gradient, and field emission was extremely strong. Field emission and gradient problems were solved by optimizing the assembling procedures. Power couplers preparation was also optimized and all antennas were electropolished.

From this point, and for all SPIRAL2 cryomodules, all components connected to the beam vacuum were checked against dust contamination using particle counters. Pumping and vesting speeds controls were hardened and high beta cavities HP rinsed twice before installation inside the cryomodule. All troubleshooting and optimization performed on high beta cryomodules is depicted in more details in references [10] and [11].

### CAVITIES AND CRYOMODULES PERFORMANCES

A detailed analysis of low and high beta cavities and cryomodules performances achieved in terms of accelerating field, quality factor  $Q_0$ , X-ray emission, thermal losses and pressure sensitivity is presented in Ref. [7]. We will in the following only recall briefly the most important results.

### Cavities

All SPIRAL2 cavities were qualified first in VC. During these tests, these cavities performances proved to be very homogeneous. They all met the project objectives (no more than 10 W of RF losses at 6.5 MV/m accelerating gradient). The measured  $Q_0$  vs.  $E_{acc}$  curves in VC are shown in Fig. 6 for low beta cavities, and Fig. 7 for high beta cavities. Mean  $Q_0$  value achieved for low beta cavities in VC is  $1.0 \times 10^9$  at 1 MV/m gradient and  $5.9 \times 10^8$  at nominal gradient of 6.5 MV/m. For high beta cavities, mean  $Q_0$  value achieved in VC is  $8.2 \times 10^9$  at 1 MV/m and  $3.7 \times 10^9$  at 6.5 MV/m.

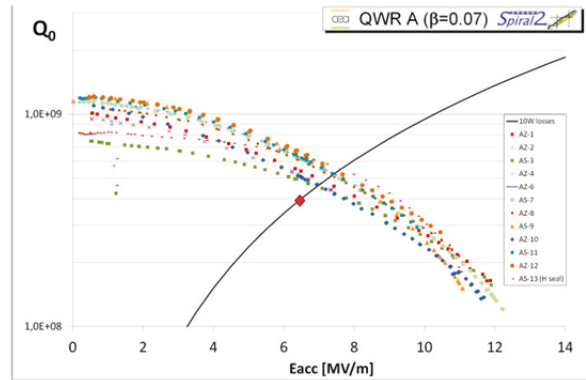


Figure 6:  $Q_0$  vs.  $E_{acc}$  curve for low beta cavities.

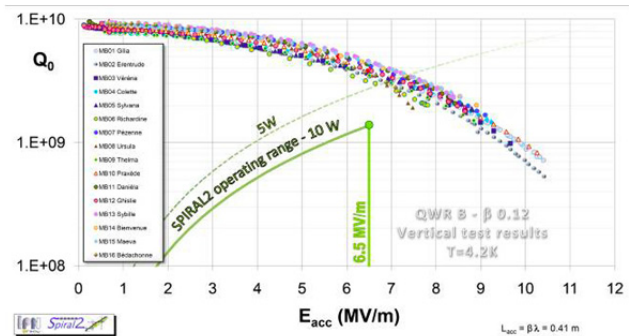


Figure 7:  $Q_0$  vs.  $E_{acc}$  curve for high beta cavities.

Table 3: Computed Ratios of Surface Fields to Accelerating Gradient

	low beta cavities	high beta cavities
$E_{peak} / E_{acc}$	5.4	4.8
$B_{peak} / E_{acc}$ [mT/(MV/m)]	8.7	9.4

Max gradient achieved in vertical cryostat is around 15% higher for low beta than for high beta cavities, which roughly corresponds to the peak magnetic field to gradient ratio difference (8%), see Table 3.

Although cavities have been manufactured by three separate companies (SDMS from France and Zanon from

Italy for low beta cavities; RI from Germany for high beta ones), no performance difference is observable.

**Cryomodules**

Performance measurements of cavities in cryomodule conditions are much less precise than in VC. Calibration is tricky and coupling factor is high ( $5.5 \cdot 10^5$  for low beta cavities and  $1.1 \cdot 10^6$  for high beta ones), so RF losses in cavities can only be estimated by cryogenic measurements [10]. Thermal losses are measured with RF power off then with RF power on, either by measuring the return gas flow or by closing input cryogenic valves and measuring the helium level decrease in buffer. The difference in cryogenic consumption is obviously giving RF losses inside the cavity. The precision of this measurement is estimated around 30% for gas flow measurements, and around 20% for helium level ones. It has to be noted that cavities installed in cryomodules have not been pushed much beyond an 8 MV/m administrative gradient limit, defined as safe for cavities, but we can assess that for all but one cavity, cryomodule operation does not lead to a significant loss of maximum gradient.

Our thermal loss measurements indicate about 15% lower mean  $Q_0$  between tests in VC and in cryomodules for low beta family, and about 30% lower in cryomodule for high beta. This is at the limit of accuracy of thermometric measurements, and could be influenced by differences in design and differences in cavities treatment before their integration inside the cryomodules. In any case, all cryomodules but one are consuming less cryogenic power than the project objectives (see Fig. 8 and Fig. 9). Static cryogenic losses estimations proved to be very reliable for low beta cavities. The best cryomodule is performing to these specs, while the mean cryomodule is less than one third above these estimations. Performances are further from the expectations for high beta cryomodules, but they remain below the target value thanks to the low RF consumption of the cavities.

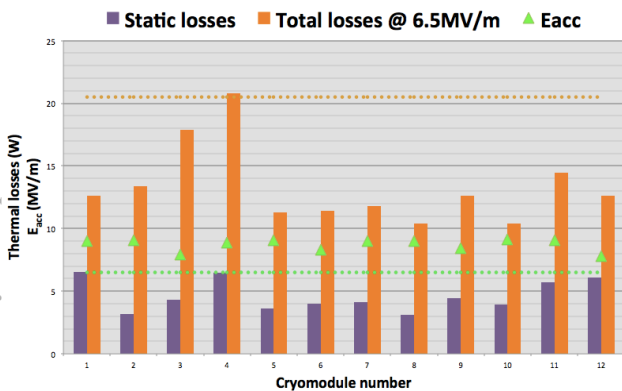


Figure 8: Cryogenic losses and max accelerating field of low beta cryomodules at 4 K. Orange dotted line indicates the total thermal loss goal of 20W, and green dotted line the goal for  $E_{acc}$  of 6.5 MV/m.

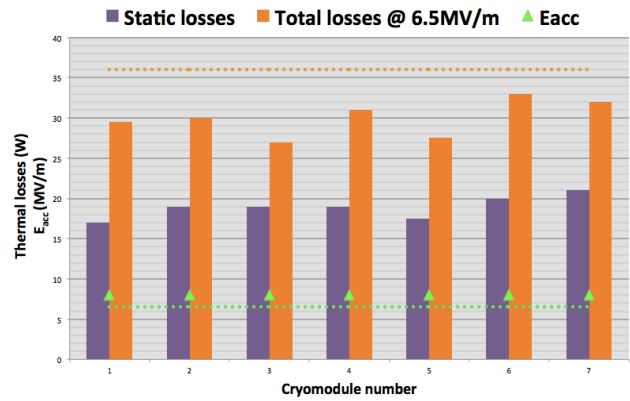


Figure 9: Cryogenic losses and max accelerating field of high beta cryomodules at 4 K. Orange dotted line indicates the total thermal loss goal of 36W, and green dotted line the goal for  $E_{acc}$  of 6.5 MV/m.

Table 4: X-ray Dose Rate of SPIRAL2 Cavities (in  $\mu\text{Sv/h}$ )

Conditions	value	low beta cavities*	high beta cavities**
In vertical cryostat, at nominal gradient	min	0	0,1
	max	2,1	4 970
	median	0,1	1,7
	mean	0,4	660
In cryomodule, at nominal gradient	min	1,4	0
	max	730	22 000
	median	293	0
	mean	325	2 223

\*Probe on top of cavity in vertical cryostat, close to the beam axis in cryomodule operation.  
 \*\* Probe close to beam axis in both tests conditions.

The X-rays dose rates emitted by cavities have been measured during VC tests and during cryomodule qualification. For high beta cavities, acquisition is always done in the direction of maximum emission, while for low beta cavities, although it is also done so during cryomodules test, the VC design forbids such a probe's position. Table 4 summarizes the results for both families of cavities. They are difficult to compare from one cavity family to another because of the difference of setup and of probe, but their general behavior is very different. Low beta cavities have a homogeneous behavior, especially in cryomodules, while high beta cavities are more "all-or-nothing". One reason is certainly related to the fact that high beta cavities have been high pressure rinsed between VC test and cryomodule assembly phases, while the low beta ones have not. Therefore there is no memory effect in the case of the high beta cavities. On the opposite, low beta cavities emitting significantly in VC still do so in cryomodules.

It proved difficult to achieve design coupling for the power coupler ( $Q_i$  factor), especially for low beta cavities (see Table 5). Both computations and room temperature RF tests with series power coupler and cavities were

performed to optimize the penetration depth of the antenna. In the end, low beta cavities are slightly less coupled than planned while high beta cavities are slightly more.

Table 5: Achieved Coupling Factor and Pressure Sensitivity Compared to Target Values

Data	Value		low beta cavities	high beta cavities
$Q_i$	target		5,5E+05	1,1E+06
	achieved	min	6,7E+05	8,4E+05
		max	1,0E+06	1,0E+06
		mean	7,7E+05	9,2E+05
Pressure sensitivity [Hz/mbar]	Target		> - 8.0	> - 8.0
	computed		- 2,5	- 7,0
	achieved (in cryomodule)	min	-2,9	- 7,3
		max	- 1,1	- 4,5
		mean	- 1,5	- 5,4

Simulations proved pessimistic as far as pressure sensitivity to helium pressure variation is concerned (see Table 4). This parameter is mainly driven by the thickness of the cavity top torus, connecting the stem to the cavity body. Therefore, difference of behavior from one cavity to the other can not only be attributed to manufacturing dispersion (these parts are deep drawn, not machined), but also to BCP chemistry “intensity”. Indeed, coarse frequency tuning has been done by chemistry, and therefore some cavities have seen longer chemical attacks than others, and have thus thinner top torus than others.

The measured performances of the cavity tuning systems in cold tests in cryomodule configuration are summarized in Table 6. The plunger tuning system used on high beta cavities was initially showing “negative hysteresis” [9]. After one year of additional tests, the problem has been understood and cured [12].

Table 6: Achieved Tuning Parameters for Both Cavity Types

Parameters (units) (specs)	Low $\beta$	High $\beta$
Range (MHz) (88.049-88.055)	In spec	In spec
Sensitivity (kHz/mm)	26.9±1.5	1.1
Hysteresis (Hz) (<20)	<4	20±12

## STATUS OF CRYOMODULES INSTALLATION



Figure 10: Low beta cryomodules installed on LINAC.



Figure 11: High beta cryomodules installed on LINAC.

All SPIRAL2 cryomodules have been produced and qualified, and are now in installation phase on the LINAC at GANIL (Fig. 10 and Fig. 11). So far, three low beta and four high beta cryomodules have been installed on the LINAC, aligned, connected to the cold valve boxes and pressure tested.

The next critical step to start soon is the connection of the cryomodules to the inter-cryomodule warm sections. It will be performed using a moveable laminar flow to cover the area and avoid any possible contamination of the cavities. A connection test has been successfully performed in Orsay, using a qualified high beta

cryomodule, to demonstrate that this operation does not degrade the cavities performances.

## CONCLUSION

Despite its reduced number of cavities (26), the SPIRAL2 project provides some interesting information regarding the achievable performances of QWR cavities in terms of surface peak fields,  $Q_0$ , thermal losses, etc.. After lengthy prototyping and pre-series phases, the achieved performances turn out to be mostly within specifications, and can serve as a guide for future LINAC designs involving QWR as to what performances can be achieved. One should nevertheless not forget that these cryomodules have yet to be put into operation on the SPIRAL2 LINAC, final performances could turn out to be slightly lower than these on the tests stands, and therefore some more design margins need to be taken into account.

## REFERENCES

- [1] [http://www.ganil-spiral2.eu/?set\\_language=en](http://www.ganil-spiral2.eu/?set_language=en)
- [2] P. Bertrand et al., "Beam dynamics and error studies of the SPIRAL2 driver accelerator", Linac'08, Victoria, September 2008.
- [3] Y. Gomez Martinez, "SPIRAL2 10 kW CW RF Coupler Design and Test", LINAC'08, Victoria, September 2008.
- [4] G. Devanz, "SPIRAL2 Resonators", 12<sup>th</sup> SRF Workshop 2005, Cornell University, July 2005.
- [5] P.-E. Bernaudin et al., "Design of the low beta, quarter-wave resonator and its cryomodule for the SPIRAL2 project", EPAC'04, Lucerne, July 2004.
- [6] G. Olry et al., "Development of a beta 0.12, 88 MHz, quarter wave resonator and its cryomodule for the SPIRAL2 project", SRF'05, Ithaca, July 2005.
- [7] P.-E. Bernaudin et al., "SPIRAL2 cryomodule production result and analysis", LINAC'14, Geneva, August 2014.
- [8] P.-E. Bernaudin et al., "Status of the SPIRAL2 superconducting LINAC", IPAC'10, Kyoto, May 2010.
- [9] P.-E. Bernaudin et al., "Assembling, testing and installing the SPIRAL2 superconducting LINAC", IPAC'13, Shanghai, May 2013.
- [10] D. Longuevergne et al., "Troubleshooting and performances of Type-B SPIRAL2 series cryomodule", LINAC'14, Geneva, August 2014.
- [11] G. Olry et al., "SPIRAL2 cryomodules B test results", SRF'13, Paris, September 2013.
- [12] D. Longuevergne et al., "A cold tuner system with mobile plunger", SRF'13, Paris, September 2013.